EUROPEAN ORGANIZATION FOR NUCLEAR RESEARCH

PS-RF-Note 009-00
CERN-NUFACT-NOTE 24
15 March 2000

Beam Dynamics in the Superconducting Section of the SPL[1)] (120MeV - 2.2 GeV)

Frank Gerigk

Abstract

After the decomissioning of LEP-2 a considerable amount of RF hardware becomes available and can be used for the construction of a high current superconducting proton linac [1]. The present design of the SPL uses four types of superconducting cavities (β=0.52, 0.7, 0.8, and LEP) to accelerate a pulsed beam of 70 mA from 120 MeV up to 2.2 GeV. In this paper a beam dynamics layout for the superconducting section is presented. The layout is optimized to keep the overall linac length short and to ensure a stable steering of the beam. Multiparticle simulations have been carried out to analyse the proposed focusing structure, and to investigate emittance growth for the nominal case and for a mismatched input beam.

[1)] Superconducting Proton Linac

1 The Linac Design

1.1 Layout

The superconducting part of the SPL is operating at 352 MHz and employs elliptical cavities with relative design velocities of β=0.52, 0.7, 0.8, and β=1.0 (LEP cavities). For the time being the maximum bunch current is set to 70 mA.[1)] Transverse focusing is provided by 1m long doublets of normalconducting quadrupoles. The choice for the basic layout parameters that are proposed (Table 1) will be explained in the following.

Table 1: Layout data

beta	**W$_{in}$ [MeV]**	**W$_{out}$ [MeV]**	**material**	**Gradient [MeV/m]**	**sync. phase [deg]**	**cells/ cavity**	**cavities/ f. period**	**foc. per. [m]**	**length [m]**
0.52	120	232	Nb	3.5	-25	4	3	6.76	94.6
0.7	232	393	Nb/Cu	5	-20	4	4	9.46	85.2
0.8	394	1063	Nb/Cu	9	-15/-10	5	4	12.29	147.6
1.0	1063	2235	Nb/Cu	7.5	-15	4	4	12.29	356.7

1.2 Design

Several constraints are narrowing down the choice for the different beta values. First of all β=0.8 was chosen because of the length of the existing LEP cryostats. These tanks can either house four 4-cell LEP cavities or four 5-cell β=0.8 cavities. Secondly, β=0.7 seems to be the lowest value, that is feasible using the niobium sputtering technique [2]. Eventually, the low energy end of the linac has to be built with bulk niobium cavities. In order to obtain a high beta value for this section, the input energy was shifted from 100 MeV [1] to 120 MeV. Moreover, 120 MeV is the threshold for the production of nuclear cascade neutrons, when protons hit the vacuum chamber. Since particle losses can be expected at the transition between the preceding drift tube linac and the superconducting structure, it is desirable to make the transition below this threshold in order to keep the activation of the machine as low as possible.

A high geometric beta (β=0.52) for the cavities of the first section is favourable for two reasons: the first one being that one can expect a much lower Lorentz Force Detuning Constant (according to [3] one can expect almost a factor of two), and the second one being the achievement of a low phase slippage. The value of β=0.52 was finally chosen to obtain a symmetric phase slippage at both ends of this section.

Since there is no experience with bulk niobium cavities for 352 MHz and since the behaviour of these cavites in pulsed mode can hardly be predicted, the accelerating gradient for this section was set to a conservative value of 3.5 MV/m. This value favours not only a small Lorentz Force Detuning Constant but is also a good choice for the longitudinal transition between the first and the second section.

[1)] this number is likely to be changed during the ongoing SPL study

Similar constraints apply for the number of cells per cavity. Five cells per β=0.8 cavity are necessary to make use of the LEP cryostats. The aim of small phase slippage, especially in the beginning of the linac, finally confines the number of cells for the β=0.52 and β=0.7 cavities to four (see Table 2).
The main criterion for the chosen transition energies between the sections, is keeping the linac length as short as possible. For this purpose the effective accelerating gradient for the different cavities was compared.[2)] This gradient refers to the energy gain of the synchronous particle passing a multicell cavity including the adjacent drift tubes. It takes into account the transit time factor (and therefore the phase slip), the nominal gradient, the synchronous phase, and the influence of the drift tubes on the accelerating fields. Fig. 1 shows the effective accelerating gradient for all four cavities and Table 1 lists the resulting transition energies.

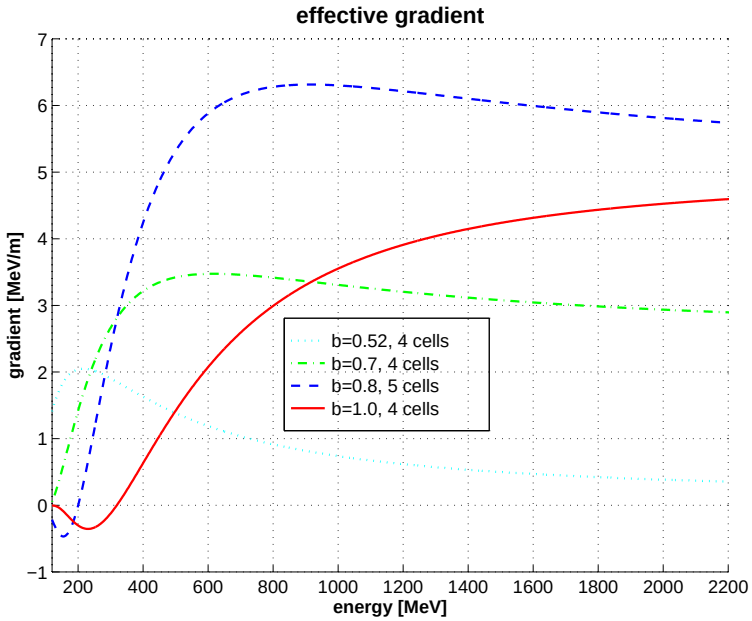

Figure 1: Effective accelerating gradient

The number of cavities per focusing period is chosen with respect to the acceptable number of $\beta\lambda$'s per period. With the exception of the last section the maximum focusing length per period rises for consecutive sections; from 17 $\beta\lambda$ for the β=0.52 section up to 20.5 $\beta\lambda$ for the β=0.8 section (Fig. 2). The jump for the transverse focusing between the β=0.52/0.7 sections and the β=0.7/0.8 sections is about 5$\beta\lambda$ in each case. As the same cryostats are used for the β=0.8 and β=1 cavities, there is no jump between these sections. This means that there are only two main sources for transverse mismatch in the linac. Altogether we end up with three cavities per period for the $\beta = 0.52$ section and four cavities per period for the remaining sections. This choice results in focusing lengths of 6.8, 9.5, 12.3, and 12.3 m in between the doublets.

[2)] SUPERFISH calculations

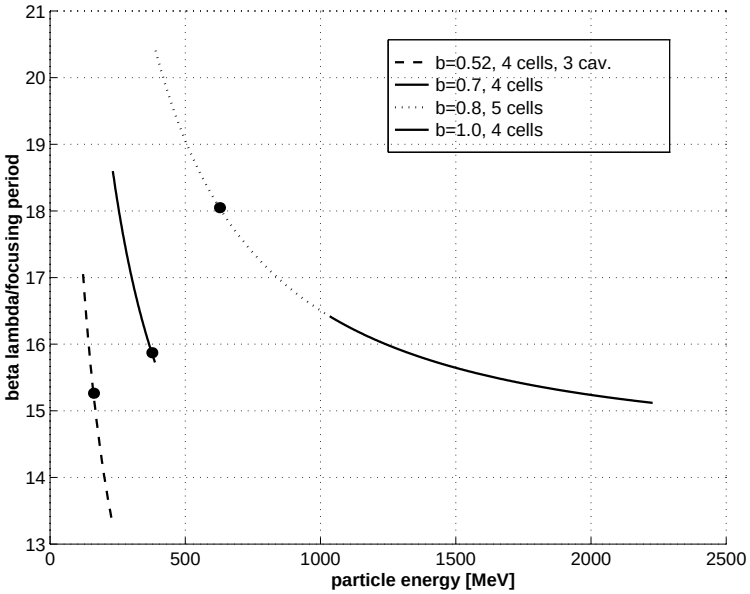

Figure 2: $\beta\lambda$ per focusing period (the dots are marking the design energy of each section)

2 Simulation Results

Initial simulations have been performed with the envelope code TRACE 3-D [4]. Later on TRACE 3-D was used to calculate the initial rms beam Twiss parameters and to match the transitions between the different sections. The matching between sections is done by changing the quadrupole gradients of four doublets in the transition area and by changing the average phase of the RF cavities.

Multiparticle simulations were carried out with the latest version of PARMILA [5] using a 6-D waterbag distribution with 50000 particles.

The magnet gradients vary between 5.6 T/m and 8 T/m. Using a doublet length of 1 m and taking into account a bore radius of 10 cm, these gradients result in pole tip fields below 1T. The gradients are adjusted so that the zero current phase advance is decreasing from 87^o for the first period down to 28^o for the last one (Fig. 3). Among the different philosophies that were tested to vary the phase advance, the present one showed the smallest emittance growth and the most stable behaviour against mismatch.

The radius of the beam pipe, that connects the cryostats and that extends through the quadrupoles has been set to 100 mm. This results in a ratio between the aperture and the rms beam size[3)] which is bigger than 27 for the whole superconducting part of the linac. At the end of the linac this ratio reaches a value of about 40. Apart from that the pipe radius is still small enough to enable the use of normalconducting standard quadrupole magnets. In Fig. 4 we can see the results for the rms and the total beam sizes along the linac.

[3)] Using the emittance values of Table 3

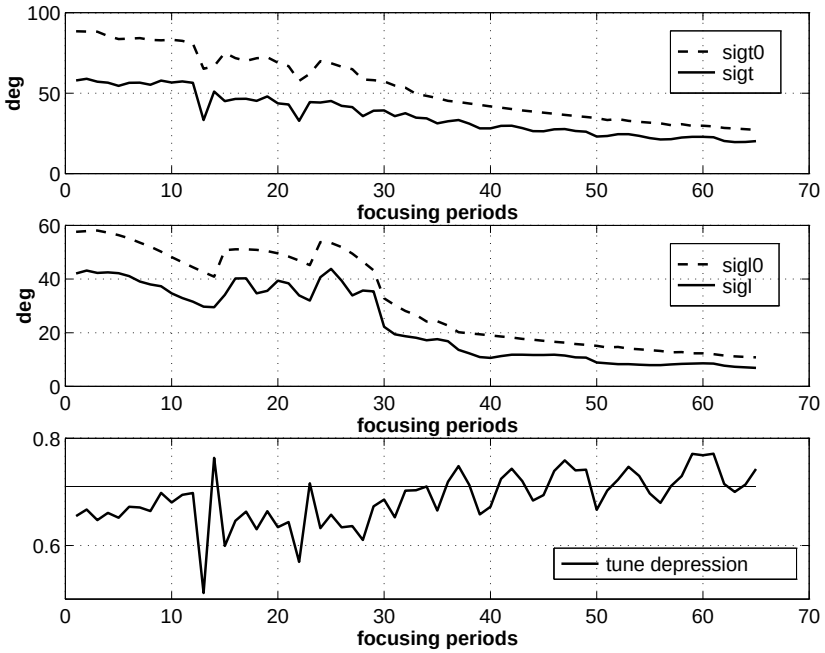

Figure 3: Top to bottom: transverse and longitudinal phase advance per period; tune depression (transverse)

2.1 Nominal case

Fig. 4 shows the evolution of the transverse beam size and Fig. 5 the energy and phase spread along the linac. We can see the beam size oscillations in the single periods as well as some residual envelope oscillations which are coming from the mismatches caused by the transitions between sections. The matching between the sections can still be optimized but the final tuning of the optics was considered beyond the aims of this study.

The amplitude of the total transverse beam size oscillations grows towards the end of linac but even the outermost particles do not exceed a radius of 1cm. This means that there is still a safety factor of 10 between the aperture and the total beam size.

The longitudinal oscillations of phase- and energy spread cool down when passing the middle of the β=0.8 section.

As shown in Fig. 6 there is practically no emittance growth, neither for the rms emittance nor for the 90% emittance. As one can see in Fig. 9 even the 99.9% transverse emittance stays stable.[4)] For the 100% transverse emittance we obtain an increase of $\approx$ 30% and the 100% longitudinal emittance grows (including the first redistribution) less than 40%. However, looking at the phase space projections (Fig. 11), one can observe the formation of beam tails in the longitudinal plane.

[4)] In the simulation there are 50 particles between 99.9% and 100%

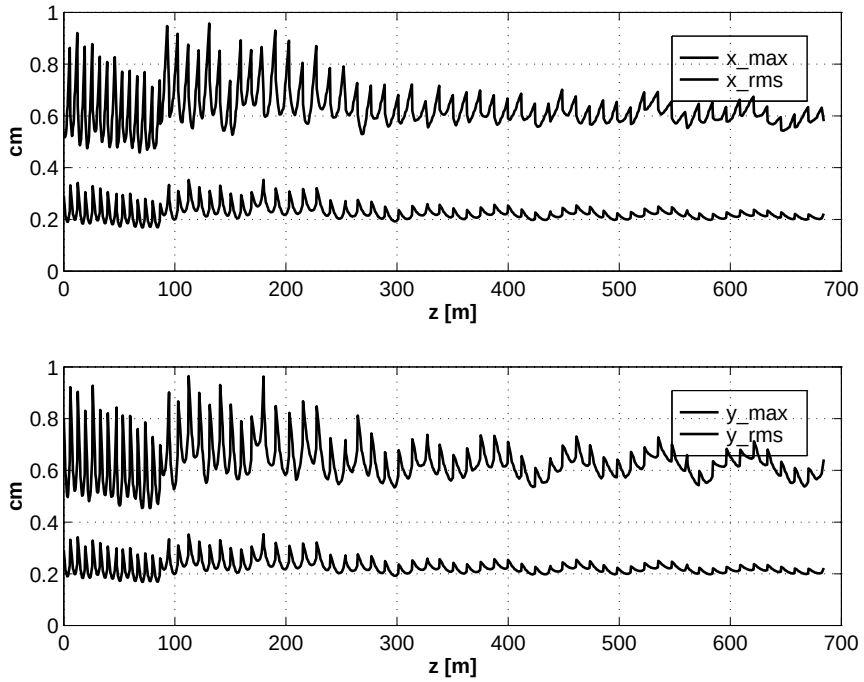

Figure 4: Transverse rms and total beam size for the nominal case

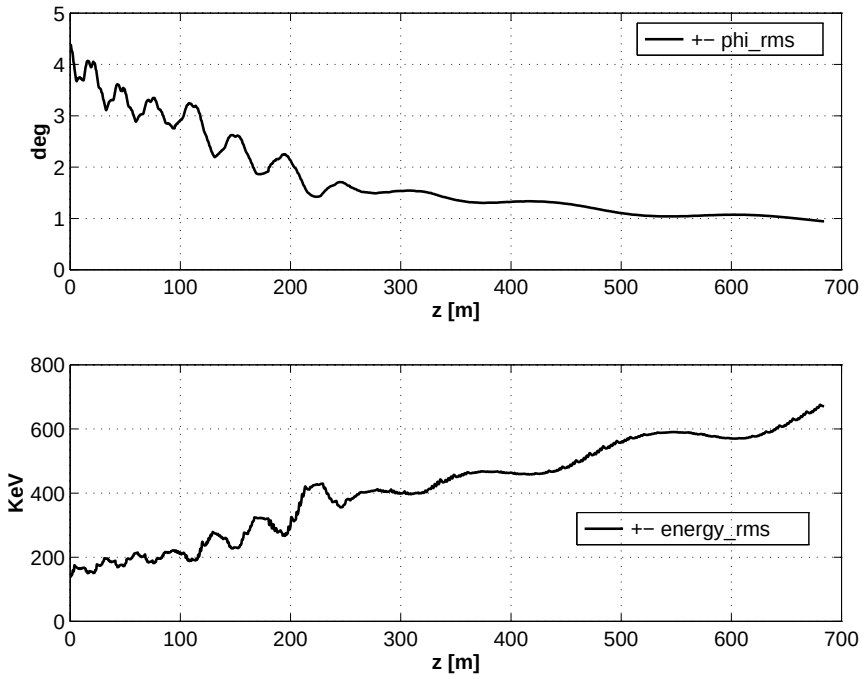

Figure 5: Energy and phase spread for the nominal case

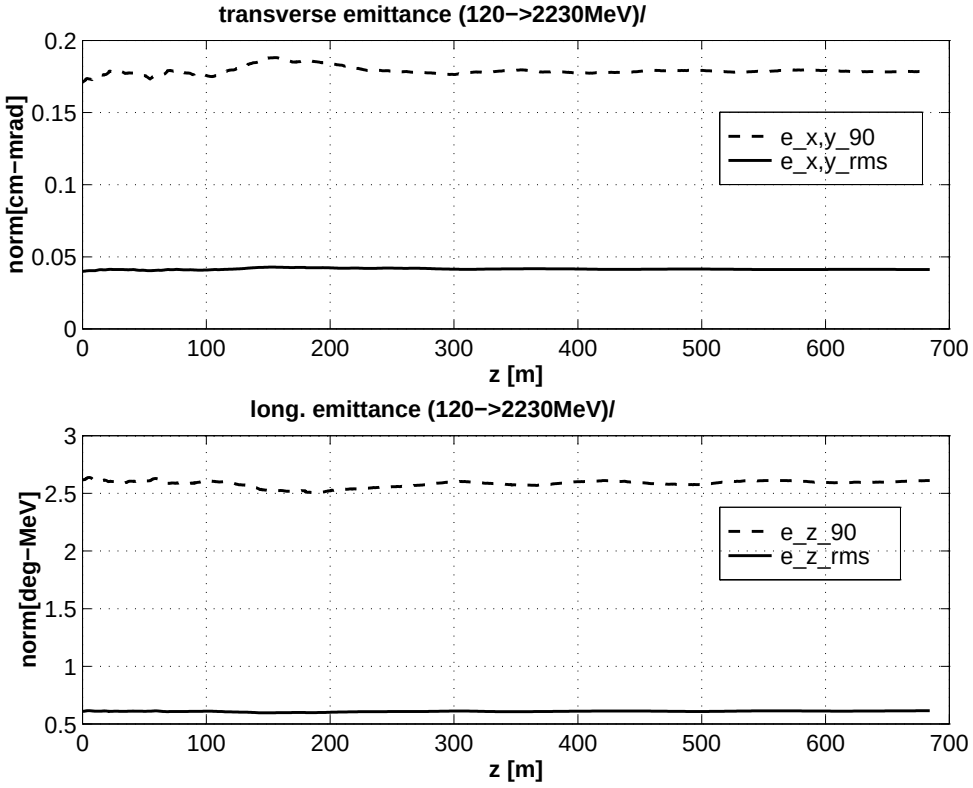

Figure 6: Rms and 90% emittance for the nominal case

2.1.1 Parametric Resonances

Looking at the condition for parametric beam resonances [6]:

$$\frac{\sigma_{t,l}^{p}}{\sigma_{env}^{Q,H,L}} = \frac{m}{n} = \frac{1}{2}, \frac{1}{3}, ... \tag{1}$$

with

$$\sigma_t \leq \sigma_t^p \leq \sigma_{t0} \qquad \sigma_l \leq \sigma_l^p \leq \sigma_{l0} \tag{2}$$

($\sigma_{t,l}$ - full current transverse/longitudinal tune; $\sigma_{t0,l0}$ - zero current t./l. tune; $\sigma_{env}^{Q,H,L}$ - envelope tunes for the Quadrupolar-, High-, and Low mode of the beam; σ^p - single particle tune)

one can calculate that the *high mode* and the *quadrupolar mode*[5)] can excite the 1/2 parametric resonance. The oscillations in beam size that can be seen in Fig. 4 are probably caused by this resonance. For the longitudinal direction one finds, that the *low mode* can excite the 1/2 parametric resonance.

The envelope tunes for all three beam modes are well below 180^o to avoid envelope instabilities and are decreasing towards the high energy end of the linac:

$$118^o \leq \sigma^Q \leq 40^o \quad 151^o \leq \sigma^H \leq 48^o \quad 92^o \leq \sigma^L \leq 16^o \tag{3}$$

[5)] the quadrupolar mode always excites transverse oscillations, since $\sigma_{env,Q} = 2 \cdot \sigma_t$

2.1.2 Equipartitioning

The input beam parameters which are taken from the previous SPL study [1] (see Table 3) are yielding an input beam that is lacking a factor of ≈5 to be equipartitioned [Eq. (4)][6].

$$\frac{\varepsilon^2_{z,rms,u}}{\gamma^2 \cdot \tilde{z}^2_{rms}} \qquad \approx \qquad 5 \cdot \frac{\varepsilon^2_{(x/y),rms,u}}{(\tilde{x}/\tilde{y})^2_{rms}} \tag{4}$$

In Fig. 7 one can see that this ratio diminishes down to one towards the end of the linac.

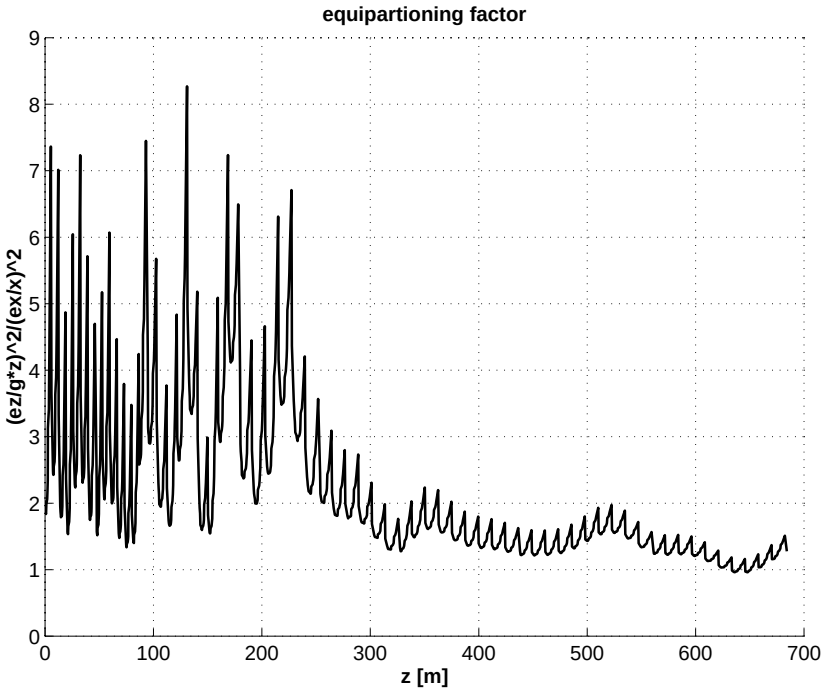

Figure 7: Equipartitioning

Although the first three sections of the linac are space charge dominated (tune depression < 0.71, see Fig. 3) the space charge factors $\delta_x, \delta_y, \delta_l$ are still relatively low (< 1).

$$\delta_{(x/y)} = \frac{\sigma_{0T}}{\sigma_T} - \frac{\sigma_T}{\sigma_{0T}} = 0.87 \qquad \delta_l = 0.64 \tag{5}$$

Which means that, according to [7]) no particular problem due to thermalisation effects is expected. Furthermore, beams with a lower equipartitioning factor were tested but without any improvement of the previous results.

2.2 Mismatched beam

In order to check the stability of the optics, a strongly mismatched beam, has been put into the linac. The presented case was simulated with 30% mismatch for the transverse and longitudinal radii of the beam, resulting in a ≈ 60% mismatch for the Twiss Parameters α and β.

[6] with: $\varepsilon_{(x,y),rms,u} = \frac{\varepsilon_{(x,y),rms,n}}{\beta\gamma}$, and $\varepsilon_{l,rms}[\pi \cdot cm \cdot mrad] = \varepsilon_{l,rms}[\pi \cdot deg \cdot MeV] \frac{\lambda \cdot 1000}{360^o \cdot mc^2 \cdot \beta\gamma}$

From Fig. 8 we can see that the transverse rms emittance grows less than 30% and that the longitudinal rms emittance grows less than 10%. For the 90% emittance we obtain $\approx$ 25% emittance growth for the transverse case and less than 5% for the longitudinal case. As we can see from Table 3 the rms beam size stays stable.
According to the simulation results none of the particles are lost in the mismatched case, meaning that no particle had a radius bigger than the assumed beam pipe.

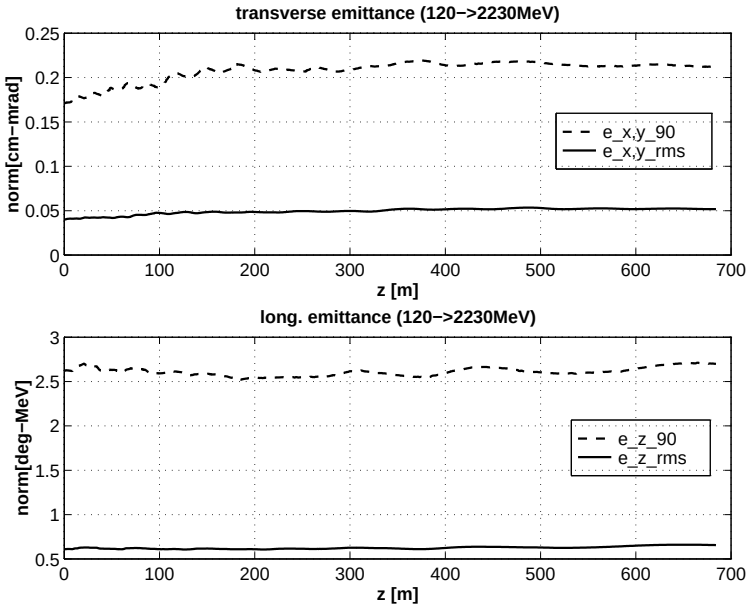

Figure 8: Rms and 90% emittance for the mismatched case (30% transverse and longitudinal)

Fig. 9 shows the emittance values for various fractions of the beam. Although the oscillations caused by mismatched particles of the beam tails are clearly visible (mismatched case), no uncontrolled blow up of the transverse emittance can be seen (even for the 99.9% emittance). This indicates, that even for this strongly mismatched case, beam losses should not exceed 0.1%, which, assuming a homogeneous loss distribution along the linac, would result in a loss ratio of a few W/m.
Regarding the phase space diagrams in Fig. 10 one can see that the introduced mismatch yields strong filamentation in the longitudinal plane and typical halo production in the transverse planes.
In order to check the effect of specific excitation of parametric resonances (see 2.1.1) the *quadrupolar mode* and the *high mode* were excited, proceeding from a 30% transverse mismatch in beam radius. Using the formulas given in [6], the corresponding input parameters can be derived from Eq. (7) and (9). The excitation of the *low mode* is rather unlikely for the presented setup and was therefore neglected, whereas the *high mode* can be excited easily. Both mismatches produced emittance growth within the range of the previously studied 30% mismatch.

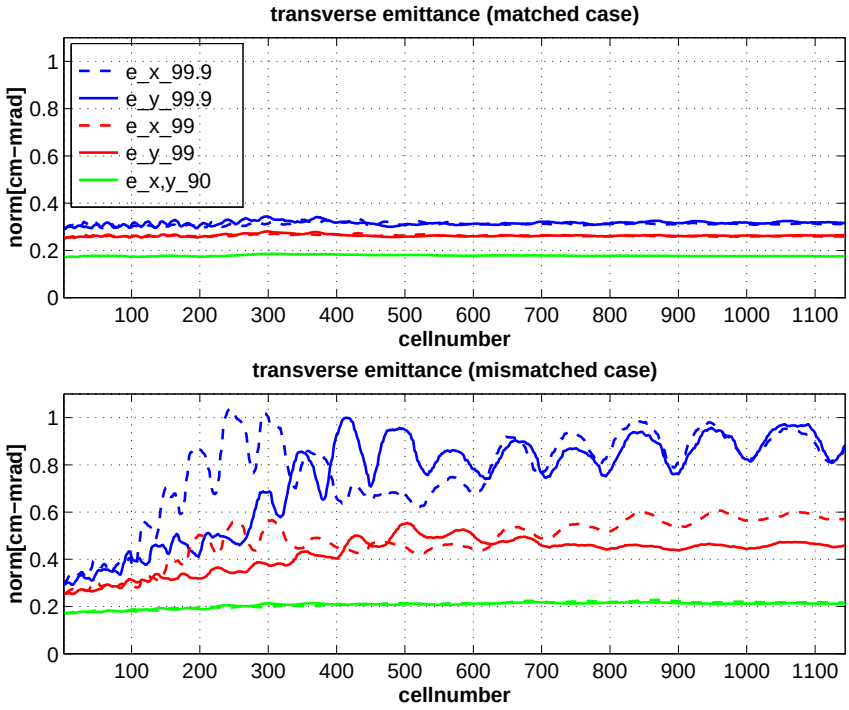

Figure 9: Emittance evolution for various fractions of the beam

quadrupolar mismatch

$$\frac{\Delta a_x}{a_{x,0}} = -\frac{\Delta a_y}{a_{y,0}} = 0.3 \tag{6}$$

$$\begin{aligned} \Rightarrow \qquad a_x &= 1.30 \cdot a_{x,0} \qquad a_y = 0.70 \cdot a_{y,0} \\ \beta_x &= 1.69 \cdot \beta_{x,0} \qquad \alpha_x \approx 1.69 \cdot \alpha_{x,0} \\ \beta_y &= 0.49 \cdot \beta_{y,0} \qquad \alpha_y \approx 0.49 \cdot \alpha_{y,0} \end{aligned} \tag{7}$$

high mode mismatch

$$\frac{\Delta a_{x,y}}{a_{x,y,0}} = g_{H,L} \cdot \frac{\Delta b}{b_0} = 0.3 \tag{8}$$

with $g_H = 9.179$ $g_L = -0.3146$ (see [6])

$$\begin{aligned} \Rightarrow \qquad \beta_{x,y} &= 1.69 \cdot \beta_{x,y,0} \qquad \alpha_{x,y} \approx 1.69 \cdot \alpha_{x,y,0} \\ \beta_l &= 1.06 \cdot \beta_{l,0} \qquad \alpha_l \approx 1.06 \cdot \alpha_{l,0} \end{aligned} \tag{9}$$

(α, β - Twiss Parameters; $a_{x,y}$ - transverse beamradii; $g_{H,L}$ - amplitude factors for High- and Low mode [calculation and derivation see [6]])

Due to the low synchronous phase, the longitudinal sensitivity against mismatch and errors is slightly higher than the transverse one. But since a low synchronous phase shortens the linac by a considerable amount, and since it is basically the transverse beam blow up that leads to activation, a higher longitudinal sensitivity seems to be tolerable.

3 Conclusion

A design for the superconducting part of the SPL has been established. The overall length of the linac could be kept short ($<$700m) by optimizing the transition energies between sections and by decreasing the synchronous phase down to -15^o towards the high energy end of the linac.

A focusing scheme has been developed, that ensures stable beam steering and that makes use of standard normalconducting quadrupoles. The multiparticle simulations of the presented linac have shown practically no increase of the rms and the 90% emittance. Mismatch studies have shown a good stability of emittance and beam size. Apart from that it seems to be realistic that the activation of the machine can be kept below the limit of 1W/m. Altogether it could be shown, that the proposed design is feasible and that the concept is promising.

For the next revision of the linac design the formation of beam halo should be studied more deeply. For this purpose one should use either a higher number of particles or a certain number of simulation runs to satisfy the statistical demands and to prove that the activation of the machine does not exceed the desired limit.

4 Acknowledgments

I want to thank M. Vretenar and A. Lombardi who introduced me to the different aspects of the SPL-dynamics, and who supervised the work for this note. I also want to thank H. Takeda from LANL for his PARMILA support.

References

[1] D. Boussard; R. Cappi; R. Garoby; H. Haseroth; C.E. Hill; P. Knaus; A.M. Lombardi; M. Martini; P.N. Ostroumov; J.M. Tessier; M. Vretenar. Report of the Study Group on a Superconducting Proton Linac as a PS Injector. CERN/PS 98-063 (RF/HP), 1998.

[2] R. Losito. Technical Development on Reduced -β Superconducting Cavities at CERN. PAC-99, CERN SL-99-024 CT, 1999.

[3] K. Bongardt. Pulsed Mode Operation of the FZJ 500 MHz sc Cavity Teststand. In *Annual Report 1999*. IKP-FZ Juelich, 1999.

[4] D.P. Rusthoi K.R. Crandall. *TRACE 3-D Documentation, LA-UR-97-886*. LANL, 1997.

[5] Harunori Takeda. *PARMILA, LA-UR-98-4478*. LANL, 1999.

[6] M. Pabst A. Letchford, K. Bongardt. Halo Formation of Bunched Beams in Periodic Focusing Systems. In *Proceedings of the 1999 Particle Accelerator Conference*. PAC, 1999.

[7] P. Lapostolle; M. Weiss. Formulae and Procedures Useful for the Design of Linear Accelerators. CERN, 1999.

Table 2: Total phase slip in the cavity end cells for the synchronous particle and for the outermost particles (in brackets)

section	**3 cells**	**4 cells**	**5 cells**
$\beta = 0.52$	$-47.4^o \rightarrow -2.6^o$	$-58.7^o \rightarrow +8.7^o$	$-69.9^o \rightarrow +19.9^o$
input	$(-70^o \rightarrow +20^o)$	$(-80^o \rightarrow +30^o)$	$(-92^o \rightarrow +42.5^o)$
$\beta = 0.52$	$-48.2^o \rightarrow -1.8^o$	$-60^o \rightarrow +10^o$	$-71.7^o \rightarrow +21.7^o$
output	$(-65^o \rightarrow 15^o)$	$(-77^o \rightarrow +27^o)$	$(-88^o \rightarrow +38.2^o)$
$\beta = 0.7$	$-50.9^o \rightarrow +10.9^o$	$-66.4^o \rightarrow +26.4^o$	$-81.8^o \rightarrow +41.8^o$
input	$(-67^o \rightarrow +27^o)$	$(-83^o \rightarrow +43^o)$	$(-98^o \rightarrow +58^o)$
$\beta = 0.7$	$-22.5^o \rightarrow -17.5^o$	$-23.7^o \rightarrow -16.3^o$	$-24.9^o \rightarrow -15.1^o$
output	$(-34^o \rightarrow -7^o)$	$(-35^o \rightarrow -5)$	$(-35^o \rightarrow -4.1^o)$
$\beta = 0.8$	$-37.9^o \rightarrow +7.9^o$	$-49.3^o \rightarrow +19.3^o$	$-60.8^o \rightarrow +30.8^o$
input	$(-49^o \rightarrow +19^o)$	$(-60^o \rightarrow +30^o)$	$(-72^o \rightarrow +42^o)$
$\beta = 0.8$	$-26.9^o \rightarrow +6.9^o$	$-35.4^o \rightarrow +15.4^o$	$-43.9^o \rightarrow +23.9^o$
output	$(-35^o \rightarrow +15^o)$	$(-43^o \rightarrow +24^o)$	$(-52^o \rightarrow +32^o)$
$\beta = 1$	$-38.9^o \rightarrow +8.9^o$	$-50.7^o \rightarrow +20.7^o$	$-82.7^o \rightarrow +32.7^o$
input	$(-47^o \rightarrow +17^o)$	$(-60^o \rightarrow +29^o)$	$(-92^o \rightarrow +41^o)$
$\beta = 1$	$-23.5^o \rightarrow -6.5$	$-27.7^o \rightarrow -2.3^o$	$-31.9^o \rightarrow +1.9^o$
output	$(-29^o \rightarrow +0^o)$	$(-33^o \rightarrow +4^o)$	$(-38^o \rightarrow +8^o)$

Table 3: Beam data for the nominal- and the mismatched beam

	in	**out**	**out (30% mism.)**	**unit**
$\varepsilon_{x,y,rms,norm}$	0.040	0.042	0.051	[π cm mrad]
$\varepsilon_{x,y,90\%,norm}$	0.17	0.18	0.21	[π cm mrad]
$\varepsilon_{l,rms}$	0.61	0.61	0.66	[π deg MeV]
$\varepsilon_{l,90\%}$	2.6	2.6	2.7	[π deg MeV]
rms beam size x,y	3.5	2.3	2.4	[mm]
rms beam size z	35	8	7.4	[ps]
energy spread	140	670	690	[keV]
phase spread	4.5	1	1	[deg] at 352 MHz

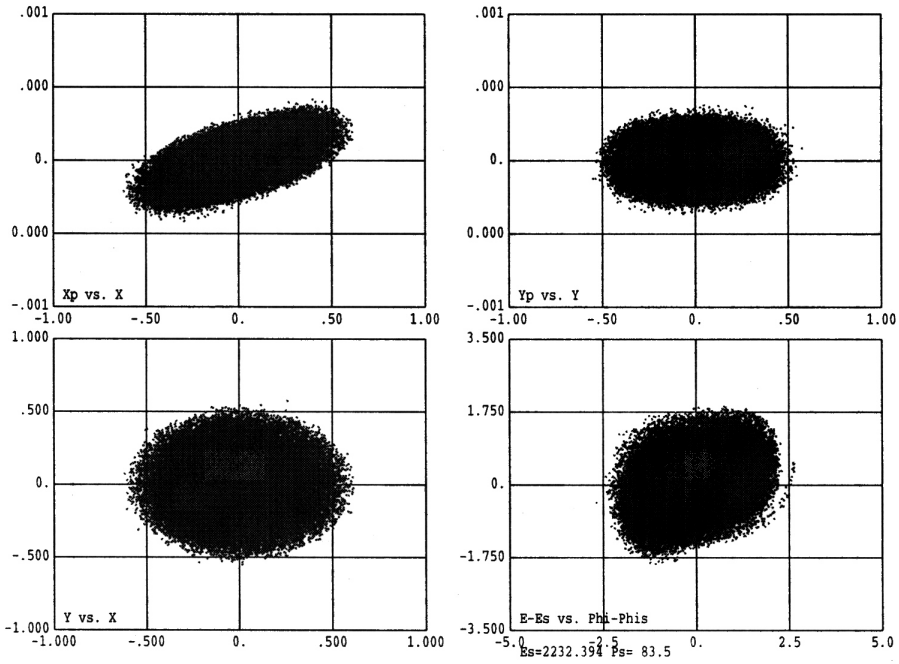

Figure 10: Emittance for the nominal case

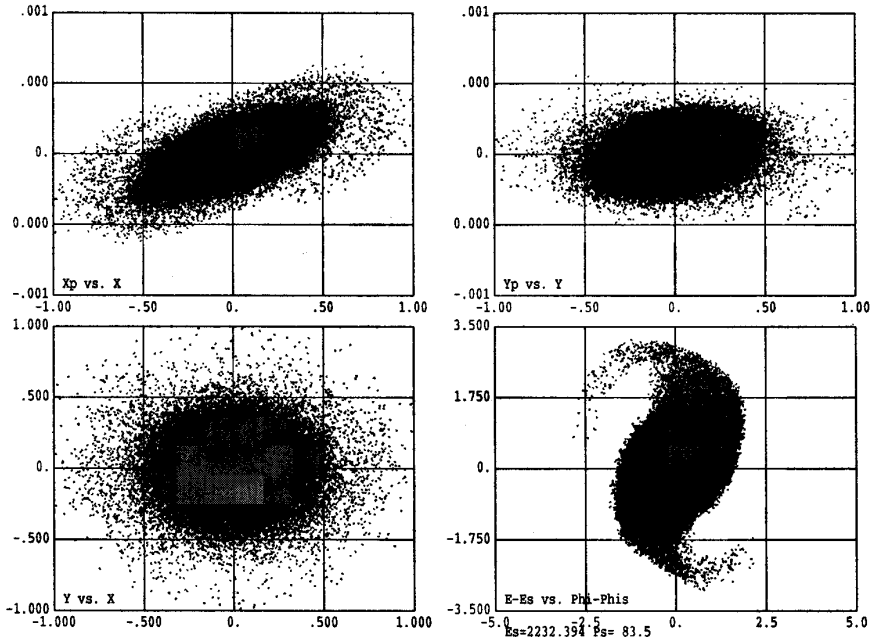

Figure 11: Emittance for the mismatched case (30% transverse and longitudinal; lower plot)